

Chapter 1

Introduction



1.1 Background

Compared with coal and oil, natural gas is clean and efficient, flexible in transportation and operation. Natural gas produces less dust, carbon dioxide and nitrogen oxides during combustion, which effectively reduces carbon emissions and mitigates the greenhouse effect [1, 2].

As an unconventional resource, shale gas exists in the shale reservoir [3, 4] as free or adsorbed. China is rich in shale gas reserves (close to 31.57 trillion cubic meters) [5, 6], mainly distributed in north China (including the Ordos and southern north China), northwest China (including Zhungeer basins) and southern China (including Sichuan Basin). At present, the Chinese industrial shale gas production area mainly includes in Weiyuan-Changning, Zhaotong and Fuling blocks [7]. The shale gas is affected by continental deposition and late transformation movement, geological conditions are complex in China. Natural gas is often detected in mountains or deserts. Earthquakes and shortages of water make the natural gas rich in the reservoir but difficult to extract, leading to high construction costs and great difficulty in exploitation [8, 9].

Hydraulic fracturing is one of the methods of mining shale gas reservoirs. During this process, high flow-rate and low viscosity fracturing fluid are injected into the strata through the wellbore, which can break down reservoir rock and facilitate migration and seepage of shale gas absorbed in the rock matrix. Due to the continuous injection of high-pressure fracturing fluid into the rock, hydraulic fractures will be created in the reservoir and will interact with preexisting interfaces in the formation, resulting in variable fracture propagation behavior (offset, arrest, crossing, branch, etc.) The propagation of subsequent fracture branches will also be disturbed by each other, which finally contributes to the formation of complex fracture networks [10, 11]. The current initial production rate of shale gas fields is only from 5 to 15% [12], far lower than expectation. Although the production has been improved by hydraulic fracturing, it is still not enough to exploit most of the shale gas. The main reason may be due to the insufficient understanding of the fracture initiation, propagation, intersection, and network formation mechanism. The current hydraulic fracture model

rarely considers the non-uniform fluid pressure effect caused by fluid viscosity and flow inside the fracture. No reliable analytical model has been established to predict the propagation path and ability of hydraulic fractures, which unfavorable fracturing efficiency of the reservoirs. Moreover, the injection of high-pressure water during the fracturing process may also reduce the effective stress in the formation, which may cause fault activation and seismic sliding. The fracture fluid flow via induced fractures easily invades and pollutes the groundwater source [13, 14]. Therefore, it is of great practical significance to study the process of hydraulic fracture initiation, propagation, intersection and network formation, to optimize the actual fracture path, intersection behavior and extension range during fracturing design and to improve the shale gas extraction rate.

1.2 Research Progress

1.2.1 *Initiation and Propagation of Hydraulic Fracture in Shale Reservoirs*

The initiation and propagation of hydraulic fracture are of great significance to the subsequent migration and exploitation of shale gas, especially the design and optimization of field construction schemes. In recent years, researchers have carried out extensive theoretical, experimental and numerical studies on the evolution of hydraulic fractures [15–17]. At present, it is mainly believed that the bonding strength and inclination of bedding planes, pore pressure, permeability, in-situ stresses, natural fracture properties, flow rate and viscosity of fracturing fluid are the main factors influencing the initiation direction, initiation pressure and propagation morphology of hydraulic fractures. The shale matrix is a tight material with ultra-low porosity (4–6%) and permeability (< 0.001 mD). Thus, fracturing fluid penetrating intact rock matrix is scarcely considered [15].

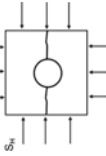
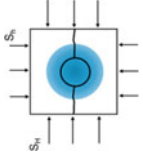
According to the linear elastic fracture mechanics, the initiation of the hydraulic fracture is consistent with the maximum principal stress direction in the homogeneous and isotropic rock. However, in shale reservoirs, the defects in shale such as bedding and microcracks are more likely distributed around the wellbore [18], which makes a hydraulic fracture first nucleate and initiate. In 1981, Huang [19] proposed a critical criterion for predicting the vertical and horizontal initiation of hydraulic fracture. He argued that the formation of hydraulic fracture depended on the stress state around the wellbore and the hydraulic fracture propagated along the maximum stress regardless of the initial fracture direction. By analyzing the surface stress of horizontal wells of shale reservoir, Guo et al. [20] proposed three modes of perforation fracturing: rock cracking, shear failure along a bedding plane (or natural fracture) and tension failure along a bedding plane (or natural fracture). Sun et al. [21] found that the bedding inclination played a critical role in the initiation of hydraulic fractures. When the bedding strength is weak and the difference between vertical and horizontal stresses

is small, the hydraulic fracture mainly initiates along the bedding plane. Considering potential microcracks distribution in the axial direction of the wellbore, Bunger et al. [22] reported that if there were multiple defects in the wellbore axis after a hydraulic fracture cracks, the fluid pressure could continue to increase [23, 24] until the occurrence of multiple-fracture initiation. Zhou et al. [25], Rongved et al. [26], Zhu et al. [27] experimentally and numerically confirmed that multiple-fracture initiation will first start from the wellbore, and the initiation process is relatively independent. Kumar and Ghassemi [28] found that the stress shadow effect can limit multiple fracture initiation, promote fracture propagation in a mixed mode of type I and type II, and inhibit the growth of surrounding cracks. Zhang et al. [29] observed that the tight arrangement of perforation clusters will lead to uneven and asymmetric hydraulic fracture.

Hydraulic fracture initiation pressure refers to the critical fluid pressure when the fracture initiation. In most engineering practices, the hydraulic fracture initiation pressure is often equivalent to the rock breakdown pressure. Determination of the rock breakdown pressure determines the economy and safety of hydraulic fracturing operations, which is of crucial importance in the hydraulic fracturing process. The rock breakdown pressure model can better explain and distinguish the physical mechanism behind the hydraulic fracture initiation phenomenon, with which the breakdown pressure can be predicted based on measured parameters. In 1957, Hubbert and Willis [30] proposed a classical breakdown pressure model (H-W model) in the tectonic stress field, after ignoring the assumption of rock permeability (Table 1.1). In 1967, Haimon and Fairhurst [31] remodified the H-W model and proposed the H-F criterion by considering the effect of fluid leak-off on the rock breakdown process. Subsequently, more new breakdown pressure models emerge and are associated with multiple parameters such as pressurization rate, fracturing fluid properties and wellbore size, forming a variety of breakdown pressure models. According to the different critical breakdown conditions, the breakdown pressure model can be categorized into a tensile strength-based method, energy release rate-based method, stress intensity factor-based method and shear failure-based method. The hypotheses applicable range the different theoretical methods are summarized in Table 1.1.

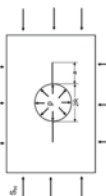
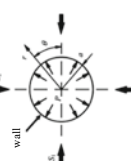
In addition to the hydraulic fracture models in Table 1.1, many models have been continuously developed and improved according to the practical fracturing treatments and prediction requirements. In 2017, Lu et al. [38] simulated the subcritical initiation and propagation of hydraulic fractures in impermeable homogeneous formations using open-hole fracturing. In 2019, Gunarathna and Silva [39] reported that vertical effective stress plays a major role in affecting the hydraulic fracture initiation pressure both for granite and shale strata. Through the analysis of the reservoir engineering data, they found that the hydraulic fracture initiation pressure increased with the vertical effective stress. In 2021, Chen et al. [40] considered the radially drilling fracturing construction and bedding orientation and established the radial drill fracture initiation pressure model of shale formation, which derived the fracture initiation pressure, the initiation direction and the location of the potential damage area. Michael and Gupta [41] compared the stress conditions in seven shale

Table 1.1 Hydraulic fracture initiation pressure models.

| Theory | Model | Authors (year) | Model overview and characteristics | Drawback |
|----------------------------------|-----------|----------------------------------|--|--|
| Maximum tensile stress criterion | H-W model | Hubbert and Willis (1957) [30] |  <p>Rock is homogeneous, linear elastic, and isotropic. Vertical stress is the minimum main stress (tectonic stress state).</p> | The rock is impermeable. Ignoring the fluid leak-off and injection rate effect. |
| | H-F model | Haimon and Fairhurst (1967) [31] |  <p>Based on the H-W model, the rock is assumed as a porous elastic medium, and the Biot coefficient was introduced to consider the fracturing fluid leakage near the wellbore.</p> | Not applicable for rocks with low-permeability. The Biot coefficient is assumed to be fixed during the fluid pressurization process. |

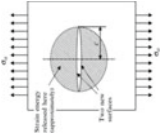
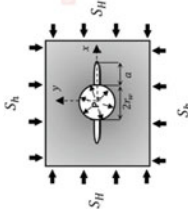
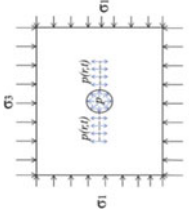
(continued)

Table 1.1 (continued)

| Theory | Model | Authors (year) | Model overview and characteristics | Drawback |
|--------|--------------------|------------------------------|--|--|
| | R-W model | Rumme and Winter (1983) [32] |  <p>Based on the H-F model, it assumes there is a pair of cracks near the wellbore with specific length α. Fracking fluid filtration and wellbore size effects are considered. Assuming that the damage occurs at the top of the characteristic crack when the maximum effective stress reaches the tensile strength.</p> | The length of the preexisting crack around the wellbore is difficult to determine. |
| | Point stress model | Ito and Hayashi (1991) [33] |  <p>Consider the effect of the (constant) pressurization rate on the breakdown pressure based on the R-W model. Stress component generated by stacking the gradient of the wellbore pressure.</p> | The mathematical solution process is very complicated, and the engineering application is limited. |

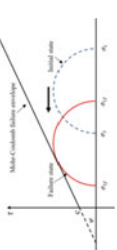
(continued)

Table 1.1 (continued)

| Theory | Model | Authors (year) | Model overview and characteristics | Drawback |
|-------------------------------------|-------------------|------------------------------|---|---|
| Griffith fracture criterion | P-K model | Perkins and Kern (1961) [34] |  | The model is only suitable for analytical linear elastic materials, limited practical application due to the determination of multiple parameters |
| Based on the stress strength factor | Rummel model | Rummel (1987) [35] |  | Formation boundary conditions and fluid infiltration effects are ignored |
| | Cracking judgment | Zhang et al. (2017) [36] |  | Complicated to be solved |

(continued)

Table 1.1 (continued)

| Theory | Model | Authors (year) | Model overview and characteristics | Drawback |
|------------------------|------------------------|-------------------------|---|--|
| Mohr-Coulomb criterion | Morgenstern model [37] | Morgenstern (1962) [37] |  <p>The fracture initiation pressure can be determined based on the known rock density, pore pressure, rock shear strength, and ambient pressure coefficient</p> | Effective stress considerations based on bulk weight are not applicable in most fracturing processes, Natural fractures, reservoir anisotropy, wellbore size, and fracturing fluid properties are not considered |

gas regions, proposed a semi-empirical method to determine the optimal perforation position and minimum ground stress, and evaluated the stress state and critical initiation conditions by using the correction factor. Among these numerous imitation pressure prediction models, current research and application are mostly based on the strength of the tension-based strength, but there is still a gap between the prediction results and the practical observation. Unknown parameters still limit engineering applications. Thus, comprehensive implementation of multiple methods should be used to obtain more reliable initiation pressure.

Fluid pressure distribution within the fracture is the internal cause that controls and affects the propagation morphology of hydraulic fracture. Fluid viscosity, flow rate and inter-joint temporary plugging can essentially affect the fluid fracture propagation state by changing the fluid pressure and its distribution form [42]. In recent decades, researchers have carried out detailed theoretical research on the resolving theoretical model of a fracture pressurized by internal fluid and obtained a series of analytical, semi-analytical, and numerical solutions, which have played a role in promoting the development of hydraulic fracturing theory to a certain extent. However, there are still gaps and deficiencies in these models compared with the real hydraulic fracturing process.

In 1921, Griffith [43] considered the effect of the fluid pressure in the fracture and obtained the stress field around a crack in a 2D infinite plane. However, the analytical solution and calculation process Griffith's is complicated. Subsequently, Sneddon et al. [44] proposed an alternative method and determined the stress field near the Griffith crack using the Westergaard stress function, but the results are still limited to the cases where the internal fluid pressure is constant. In 1997, Liu and Wu [45] adopted the Muskhelishvili complex function theory and presented an approximate analytical expression of crack opening degree (COD) (Fig. 1.1)

$$U(x', \alpha, \omega) = \frac{\sigma \omega}{E'} \left\{ \frac{4}{\pi} [C_{1pl} x' F(\omega, x') + C_{2pl} F(\omega, x')] + C_{3pl} x' + C_{4pl} \right\} \quad (1.1)$$

where, C_{ipl} ($i = 1, 2, \dots, 4$) is the predetermined coefficient, and its expression is $C_{ipl} = \sum_{p=0}^4 \left(\sum_{l=0}^4 f_{ipl} \omega^l \right) \alpha^p$, $\omega = d/a$, $\alpha = a/W$ and $x' = X/a$.

The approximate treatment of the fracture width by Liu and Wu [45] significantly improves the accuracy and efficiency of the stress field near the crack tip. However, the segment and uniform pressure distribution is not sufficient to reflect the distribution state of fluid pressure along the fracture length.

To study the hydraulic fracture initiation, researchers have established different models of hydraulic fracture, as shown in Fig. 1.2, including PKN model, KGD model and Penny-shaped model. The PKN model assumes that each vertical section is an elliptical crack in a planar strain state and that the crack height along the propagation direction is constant [46]. The maximum crack width perpendicular to the vertical profile is determined by the local fluid pressure and the confining pressure stress. This model is to simulate the one-dimensional flow of the fluid along the crack. The KGD model is assumed in the horizontal cross-section and uses Poissuille's law to

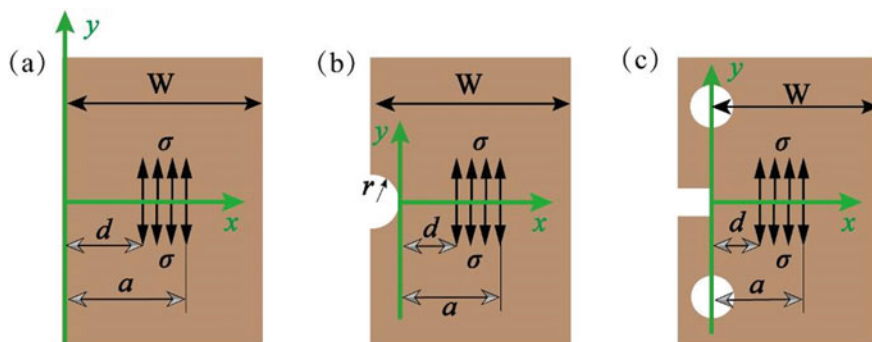


Fig. 1.1 Stress state of fracturing sample: **a** single side crack tensile sample, **b** single side band notch crack tensile sample, **c** compression tensile sample [45]

describe one-dimensional fluid flow within cracks, which describes the relationship between fluid pressure and fracture width [47]. The Penny-shaped hydraulic fracture model has a 3D axisymmetric shape extending radially around the wellbore [48]. In 2001, based on the KGD hydraulic fracture model (Fig. 1.2b), the research group of Detournay [49–52] established the relationship between the internal fluid pressure and the crack opening by coupling the fluid lubrication theory and the rock elasticity equation expressed as

$$p(x, t) = p_f(x, t) - \sigma_0 = -\frac{E'}{4\pi} \int_{-l}^l \frac{\partial w}{\partial s} \frac{ds}{s-x} \quad (1.2)$$

In addition, Detournay et al. [53] also defined two energy dissipation regimes (i.e., fluid viscosity-dominated and fracture toughness-dominated) based on different energy dissipation processes during the hydraulic fracturing process. The rock toughness response can be ignored when the viscous dissipation within the crack is dominated. In 2012, Garagash and Sarvaramini [54] categorized two types of hydraulic fracture propagation (Fig. 1.3). When the fracture length is less than the wellbore radius, hydraulic fractures are assumed as edge fractures. When the fracture is greater than the wellbore radius, the hydraulic fracture is assumed to be a Griffith crack. However, the works of Garagash and Sarvaramini [54] are only aimed at the fracture shape and critical propagation state, and the changes in the stress and displacement fields induced by non-uniform pressure fluid within the crack are not involved. In 2019, Zeng et al. [55] used the weight function and derived the analytical solution of the fracture initiation stress around the wellbore, and found that the initiation pressure subject to the nonuniform fluid pressure was higher than that under constant pressure. In 2020, Li et al. [56] divided the fluid pressure into a constant pressure section and a rapid pressure drop section based on the pressure form inside the hydraulic fracture. The approximate solution of the fracture opening under nonuniform fluid

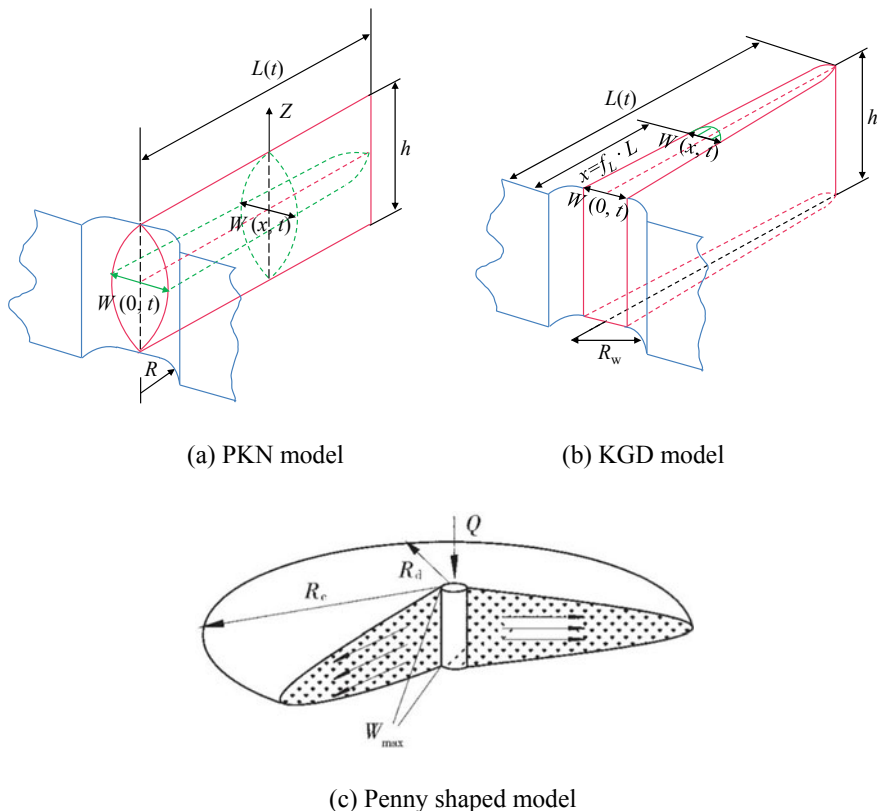


Fig. 1.2 Hydraulic fracture model in extending state

pressure is obtained by piecewise integration. The reliability of the solutions is verified by comparing the approximate solution to Sneddon’s semi-analytical solution [44]. In 2022, Wrobel et al. [57] established a simplified model for the stress redistribution around the fracture tip and introduced a plasticity-related crack propagation condition. Wrobel et al. [57] considered the plastic deformation near the fracture tip. However, their model neglects the perturbation effect of the pressure gradient on the surrounding stress field. Previous hydraulic fracturing experiments, numerical simulations, and field studies have shown that the fluid pressure gradient in rock is nonlinear [58–60], especially in the disturbance of fluid viscosity and pumping parameters. In addition, numerous experimental and simulation studies [61, 62] have also shown that the nonuniform pressure form in the fracture has an important influence on the stable state of the initial fracture, new propagation direction, and final formation of an effective fracture network.

From this point of view, it is necessary to establish a model reflecting the influence of the nonuniform pressure inside the fracture on the propagation of hydraulic fracture. Sneddon [44] suggested using a general polynomial to characterize the internal

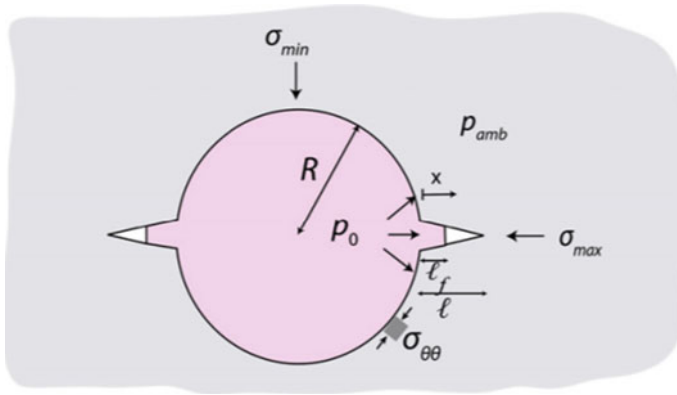


Fig. 1.3 Symmetrical crack distribution near the well bore [55]

fluid pressure e . Based on the integral transform of complex functions, the analytical form of the displacement induced by specified fluid pressure is derived. However, Sneddon [44] only gives the form solution of the displacement analytical equation and does not apply this analytical solution to determine the hydraulic fracture propagation, which has limitations in the practical engineering application. It is important to further investigate the perturbation effect of nonuniform fluid pressure on the propagation process of hydraulic fracture. The reliability of the analytical solution and its applicability to the actual fracture process can be further demonstrated by using experimental and engineering data.

1.2.2 Model of the Intersection of Hydraulic and Natural Fracture

Engineering experience [63, 64] shows that the interaction between hydraulic and natural fracture is an essential influencing factor in the formation of complex fracture networks and the intersection behaviour between fractures is the ultimate cause of high fracturing fluid filtration loss, early sand plugging, fracture propagation obstruction, fracture steering and high network pressure in the actual fracturing construction [65]. The intersection of hydraulic fracture and natural fracture involves complex effects such as flow-solid nonlinear coupling, fracture propagation, rock non-local fracture response and intersection disturbance, covering the two physical processes of hydraulic fracture gradually approaching natural fracture (extension approach) and fracture tip passivation (intersection passivation) when hydraulic fracture and natural fracture intersection. During the extended approximation process, the natural fracture stress state is disturbed by the gradually increasing fracture tip stress singularity; In the intersection passivation process, the fracture tip stress singularity has failed, and the subsequent fracture propagation is dominated by the dynamic flow

pressure of the fluid in the fracture [66]. Due to the singularity of fracture tip stress, the interaction between fractures and the extension path of fracture is different in different processes.

Some scholars have carried out a series of research based on the extended approximation process, mainly establishing the intersection criteria from the aspects of approximation perspective, critical stress state, fracture fluid pressure form, etc. In 1995, Renshaw and Pollard [67] proposed a model for the vertical intersection of hydraulic fracture and natural fracture (Fig. 1.4a): under the action of the stress field at the hydraulic fracture tip of the natural fracture, when a new fracture is produced on the other side of the natural fracture surface and the natural fracture surface does not slip, it is considered that the hydraulic fracture will pass through the natural fracture. This is an idealized either non-slip or pass-through compression crossing model, aiming at describing the perturbation effect of the fracture process region on the natural fracture, but this model is limited by the strict symmetrical vertical approximation angle, which does not show the propagation form of the inclined intersection. In 2013, Sarmadivaleh and Rasouli [68] extended the Renshaw and Pollard criteria to an arbitrary approximation angle (Fig. 1.4b) to obtain an analytical form of the compressed crossing criterion. In 2014, Zhang et al. [69] gave the calculation method for the turning Angle of hydraulic fracture through natural fractures based on Sarmadivaleh and Rasouli's works. They proposed a revised version of the intersection criterion (Fig. 1.4c) to determine the initial direction of subsequent compression through fracture propagation. The calculation results show that: when the approximate angle is constant, the horizontal principal stress ratio required for the hydraulic fracture to pass through the natural fracture is within limits. Neither too high nor too low principal stress ratios can make the hydraulic fracture pass through the natural fracture; In addition, under the large approximate angle and the horizontal principal stress ratio (maximum principal stress ratio, minimum principal stress), the hydraulic fracture tends to expand directly through the natural fracture; At the same approximation angle, the greater the horizontal primary stress ratio value, the piercing direction always tends to be close to the increased horizontal primary stress direction. Considering the matrix heterogeneity and rock mass seepage-stress-damage fracture characteristics, in 2016, Zhao et al. [70] studied the influence of natural structures of different scales. The results show that the tension damage between hydraulic fracture and nonclosed fracture directly led to penetration between fractures. If the intersection angle between the direction of the maximum principal stress and the bedding plane strike is small, the hydraulic fracture will propagate along the tectonic plane; While the direction of the maximum principal stress intersects the bedding plane at a large angle, the maximum principal compressive stress and the bedding plane simultaneously dominate the joint network propagation process. The study also confirmed that reservoir hydraulic fracture is a transient dynamic disturbance process within a local scope, but the study did not consider the disturbance effect of the stress field at the tip of the approximation process. In 2017, Llanos et al. [71] studied the influence of the hydraulic fracture vertical approach process on stability based on the change of constant fluid pressure, hydraulic fracture length, and approximation distance (Fig. 1.4d). The study shows that with the shortening of the approaching

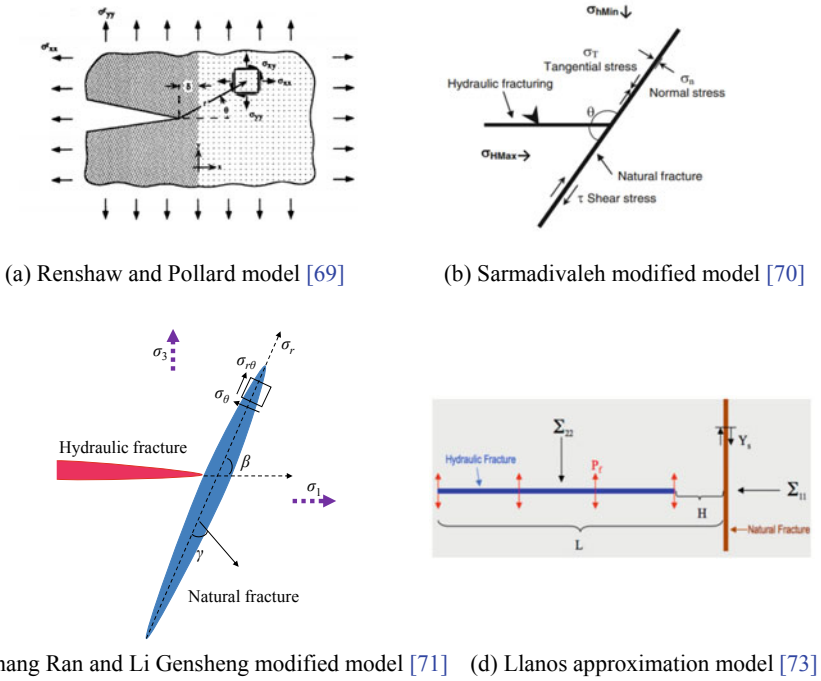


Fig. 1.4 Intersection model between a hydraulic fracture and a natural fracture based on the approaching process

distance, the stress state change on the natural fracture surface intensifies, and the natural fracture surface also tends to slip and initiate. However, Llanos’ study only considers the orthogonal approximation of the two fractures, while the change in the actual approximation angle will also have different effects on the extension direction of the natural fracture [72].

In 2018, Zhao et al. [73] extended Llanos’ approximation model to arbitrary approximation angles. They coupled it with the simultaneous fluid flow (lubrication equation) and rock elastic deformation (elastic equation), then proposed the intersection of toughness master hydraulic fracture (constant fluid pressure in the joint) and discontinuous friction interface, and clarified the disturbance law of the hydraulic fracture dynamic approach process to the stress state of any natural fracture surface. In 2019, Zhao et al. [74] introduced natural fracture critical opening conditions based on the crossing criteria and established a composite model of the dynamic approach of natural fracture in hydraulic fracture and predicting the three intersection behaviors (opening, crossing, and slip, shown in Fig. 1.5), to provide a theoretical basis for subsequent propagation behavior prediction. Janiszewski et al. [75] studied the interaction mechanism between hydraulic and natural fracture based on the fracture mechanics modeling code FRACOD simulation. They believed that a small approximation angle is beneficial to the hydraulic fracture angle and the activation

of natural fracture, which leads to the propagation of wing tensile fracture from the tip and forms a complex fracture network. Daneshy [76] established a 3D approach intersection model considering three types of natural fracture (open, closed unbound, closed bond) and found that the character of natural fractures directly affects the intersection behaviour and hydraulic fracture propagation state. In contrast, the ground stress, approach angle, and fracture fluid pressure are the main control factors leading to the activation of natural fracture. In 2020, Zeng et al. [77] proposed the criterion of type I/II mixed mode hydraulic fracture passing through the natural fracture based on the stress field around the hydraulic and the natural fracture and approached the zero simplified criterion through the composite degree (K_{II}/K_I) and applied it to the verification of the test results. In 2021, Zhu and Du [78] proposed a critical criterion for hydraulic fracture passing through natural fracture based on fracture tip T-stress. They found that T-stress always limits the direction change of hydraulic fracture when passing through the natural fractures interface. Zhao et al. [79] established a 3D intersection model of hydraulic and natural fracture and verified the prediction model combined with indoor experimental data. They also qualitatively summarized six types of intersection behaviors: crossing, sliding and initiation, initiation, sliding, sliding plus crossing and arrest. Unfortunately, only two kinds of crossing and slip were observed in Zhao's tests [79], and the test basis for the six types of intersection behaviors was not found. Also, the critical conditions and order for the occurrence of the six types of intersection behaviors were not given. There are only three independent intersection behaviors in the hydraulic approximation process theoretically (Fig. 1.5). Once the natural fracture slip, the stress state around the natural fracture will change, affecting the following propagation state of the fracture. In 2022, Zheng et al. [80] believed that the interaction of non-intersecting fracture in the propagation process could not be ignored. The inter-fracture interaction model was established based on the boundary element and rock fracture criteria and found that natural fracture could cause at least 22° deflection under appropriate conditions.

Most of the previous intersection standards based on the approximation process have ignored the effects of fluid viscosity and flow rate. The fluctuations in the fluid viscosity and the injection rate during the actual hydraulic fracturing process cause changes in the in-fracture fluid pressure with time and fracture length. The

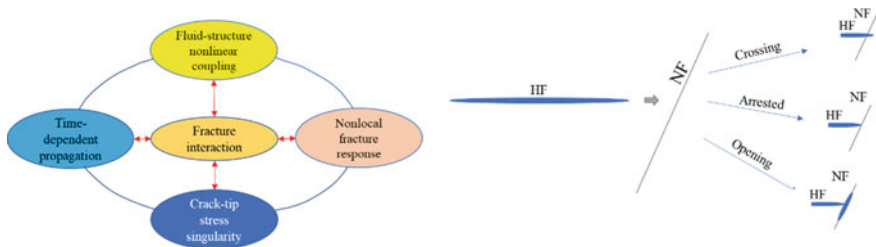
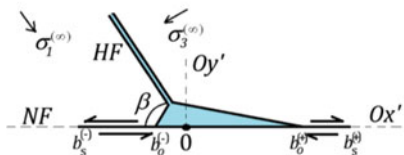


Fig. 1.5 Intersection behavior between a hydraulic fracture and a natural fracture

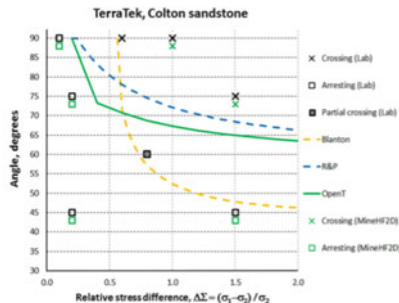
hypothetical fluid pressure is invalid, and the coordination criteria of the tough main control hydraulic fracture are no longer applicable.

The study of intersection criteria for intersection passivation processes goes from qualitative analysis to quantitative computation. In 1986, Blanton [82] simplified the forming of natural fracture shear stress distribution. Based on the critical fluid pressure conditions in the fracture after intersecting passivation, the culinary stress component of the rock resistance and geological stress component was qualitative. However, the judgment only considers the critical condition of fracture crossing and ignores the disturbance effect of the propagation state fracture induction. In 1987, Warpinski and Teufel [83] superimposed the stress field and supplemented the critical stress conditions of natural and hydraulic fracture after passivation and intercourse. However, it is still limited to the interaction of the fracture tip and the grounding force field. The fluid pressure effect, natural fracture penetration, and the position and direction of the new fracture after passivation is not considered. In 2014, Chuprakov et al. [81] established a fracture tip passivation model considering the influence of rock fracture toughness, hydraulic fracture length, natural fracture permeability, and the effect of injection rate (Open T model, shown in Fig. 1.6a). It described the partition characteristics of the natural fracture opening and sliding segments of the fracture tip passivation zone, determined the orientation of the new nucleation fracture, and described the natural fracture activation problem quantitatively. Considering the type of T-type passivation contact form, in 2015, Chuprakov and Prioul [84] established the friction sticky interface of natural fractures on fracture high control effects (FRACT models) and applied the criteria to the 3D bedding rock stream coupling model simulation, and analyze the high control mechanism of natural fracture on hydraulic fracture. In 2019, Xu [85] considered hydraulic fracture fluid lag area effect and fracture tip passivation using analytical and numerical (noncontinuous deformation analysis) way to establish the hydraulic and natural fracture intersection model which mainly predicts the fracture tip to natural fracture and fluid front did not contact with natural fracture, hydraulic fracture crossing the natural fracture. It was found that hydraulic fracture is easier to cross natural fracture under large crustal stress, approximation angle, interface friction, injection rate, and fracturing fluid viscosity. In 2020, Zhao et al. [86] investigated the intersection mechanism of hydraulic and natural fracture with different shear strengths based on the 3D lattice-spring method. The results show that the tensile strength of the intact fracture and the shear strength of the joint play a dominant role in the intersection behavior between the two fractures. However, the intersection criteria and models of the fracture intersection passivation process described above ignore the perturbation effect of the hydraulic fracture tip stress singularity, which is particularly significant in the two-fracture propagation approximation process.

In general, the intersection process of hydraulic fractures and natural fractures is affected by rock mechanical properties (elastic modulus, fracture toughness, tensile strength, etc.), natural fracture mechanical properties (shear strength, interface friction coefficient, cohesion, etc.), fracturing fluid flow and viscosity, approach angle, crustal stress difference, etc. The approximation process of the intercourse is rarely involved in the non-average pressure flow effect of the fracture caused by fluid



(a) Open-T model



(b) The behavior predicted by the model

Fig. 1.6 Open-T model and its predicted fracture behavior [81]

viscosity and flow velocity changes. Therefore, it is not considered that the disturbance of the stress field of dynamic changes around the surrounding dynamic changes in the actual hydraulic fracture. Monitoring data deviations are large. To further enhance the reliability of the prediction results of the interchange standards, a reasonable change in fluid pressure conditions needs to be introduced within the standard, and the dynamic propagation of hydraulic fracture and dynamic propagation of the natural fracture process of new fracture, propagation, and interchange stress thresholds. The stability change rule of the natural fracture surface is revealed to predict the subsequent intersection behavior.

1.2.3 Formation Mechanism of the Complicated Crack Network of Shale

Shale is formed by clay mineral dehydration, cement and later deposition, rich in apparent thin sheet bedding and natural microcracks [87, 88]. The combinations of different productive bedding, microcracks and other matrix defects form discrete crack systems in shale reservoirs. In the hydraulic fracturing of fractured shale reservoirs, high-pressure fluid-driven hydraulic fracture connected with the reservoir anisotropy and randomly distributed fracture clusters, branch fracture in the rock body breakdown with all kinds of fracture overlap and extension, forming a complex 3D fracture network (Fig. 1.7). Influenced by the bedding direction and the random distribution of natural fracture, the shale hydraulic pressure fracture network is diverse and discrete characteristics [89, 90]. Establishing a large-scale and interconnected complex fracture network is the key to realizing the effective extraction and commercial development of shale gas reservoirs.

Indoor hydraulic fracturing test plays a vital role in understanding the fracture propagation mechanism, studying the formation of the complex fracture networks, and simulating the field fracturing process. Based on physical model experiments and

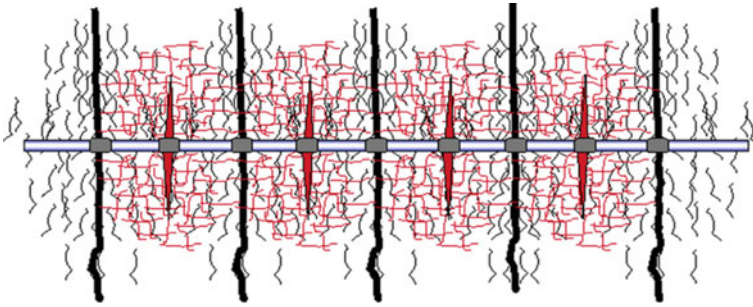


Fig. 1.7 Schematic diagram of a complex fracture network (multistage fracturing) [91]

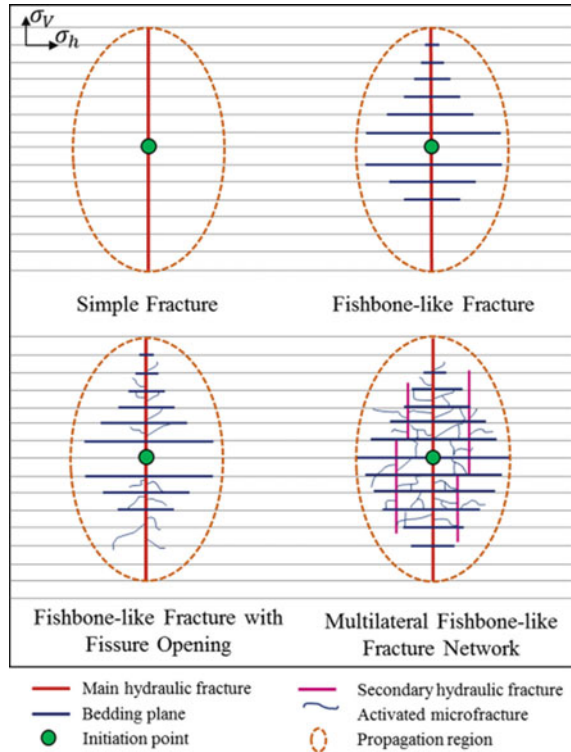
dynamic acoustic monitoring technology, scholars have carried out some research work in fracture pattern characteristics and fracturing modification [92], focusing on the analysis of the influence of stress state, fluid viscosity, pump injection flow, formation lithology, occurrence and distribution of fractures (including bedding and primary microfractures), fracturing technology, etc. on hydraulic fracture propagation path and fracture pattern.

The model experiment of studying the complex fracture mesh in shale reservoirs has undergone a transition process from rock-like materials to rock materials, prefabricated cracks to natural fractures, and visual observation to acoustic wave dynamic scanning and monitoring. Considering the influence of 3D production and ground stress in natural fractures comprehensively, in 2005, de Pater et al. [93] studied the influence of fluid properties on fracture intersection behavior with the help of fracture intersection model experiments and numerical simulation. It was found that the high-flow and high-viscosity fracturing fluid produces multiple hydraulic fractures, while the low-flow fracturing fluid tends to open the natural fractures. In 2015, Dehghan et al. [91] studied the influence of natural fracture yield and horizontal stress difference on fracture propagation with the help of the true three-axial hydraulic fracture. The experimental results show that under the condition of small horizontal stress difference, the strike and dip angle of natural fractures play a controlling role in the propagation law of hydraulic fractures. Improving the horizontal stress difference or increasing the strike and dip angle of natural fractures on the experimental scale can inhibit the poor development of hydraulic fractures. Considering the influence of the shale lamination effect, Tan et al. [94] used horizontally laminated shale test samples to carry out the true triaxial hydraulic fracturing experiment in 2017. They studied the effects of ground stress, laminar surface, injection rate, fracturing fluid viscosity, and other factors on fracture vertical propagation behavior and fracture morphology, and summarized four typical propagation modes of vertical production of laminar shale fracture (Fig. 1.8): Single fracture, fish-bone fracture, fish-bone fracture with bedding opening, and multi boundary fish-bone fracture network. Differences in the physical and mechanical properties of natural fractures are limited by changes in the sedimentary environment. In 2018, focusing on the influence of the sedimentary environment

and natural bedding on fracturing morphology, Zhao et al. [95] compared the differences in hydraulic fracturing forms of Marine shale and continental shale and gave the relationship between section roughness and stress state based with the experimental results. In 2019, Chong et al. [96] studied the effect of shale reservoir anisotropy on pressure fracture networks based on hydraulic fracturing experiments with different initial stress states and injection rates. Based on a CT scan, they explained the impact of shale anisotropy inclination on hydraulic fracture. According to the analysis of CT images and results of 3D reconstructed hydraulic fracturing samples, Jiang et al. [97] believed that the key to shale fracturing volume change was the complexity of fracture formation and the fracture propagation distance generated by fracturing, and the stress difference played a significant role in controlling the formation of the complex fracture network. Considering the effect of fluid properties, Wang et al. [98] studied the influence of fluid viscosity and flow on the fracturing effect based on the true three-axial hydraulic fracturing test of bedding shale and found that the fracturing fluid with high injection rate and viscosity mainly forms a single main crack form. In contrast, the fracturing fluid with low viscosity and low injection rate promotes the formation of a complex fracture network. Hou et al. [99] conducted an experimental study on the effect of slippery water/guar glue fusion injection on fracture initiation and propagation in deep shale gas reservoirs. The study found that guar gum tends to open transverse fractures in deep shale reservoirs. In contrast, slippery water tends to activate the surface under the temporary blocking of guar glue combined with the fracture propagation morphology, a large and complex fracture network was injected alternately with different viscous fracturing fluids.

It is of great significance to understand the initiation and geometric properties of hydraulic fractures for optimizing hydraulic fracturing design and improving the final production of shale reservoirs. In 2019, Wu et al. [100] applied the shear tensioning fracture model to the data analysis of the triaxial hydraulic fracturing acoustic emission of stratified shale and evaluated the cumulative change pattern of the test sample tensioning and shear fracture in the hydraulic fracture process, and used the average fracture inclination and initiation width index to identify the fracture morphological characteristics quantitatively. In 2020, Chen et al. [101] used the true three-axial fracturing test system to simulate the influence of the ground stratification, ground stress difference, the hydraulic fracture initiation and propagation process. They found that the hydraulic fracture is easy to extend along the bedding direction with weak cementation, and the high ground stress difference promotes the formation of a single fracture form, while the viscous fracturing fluid and temporary plugging in the front are conducive to the formation of the complex fracture network. Dehghan [102] performed a series of true three-axis hydraulic fracturing tests based on large synthetic rock samples of preformed natural fracture on the laboratory scale and studied the extended behavior and length change characteristics of hydraulic fracture in natural fracture reservoirs. They believed that ground stress is the dominant factor in disturbing fracture intersection behavior and controlling fracture propagation length. Zhang and Sheng [103] considered the influence of the power-law distribution form and spacing of natural fracture and obtained the optimal fracture

Fig. 1.8 Schematic diagram of hydraulic fracture propagation morphology in vertical plane of shale reservoirs [94]



mesh layout method of complex natural fracture reservoirs by the simulation and optimization of various complex fracture network layout methods.

In 2021, Wu et al. [104] established an evaluation model of fracture network connectivity based on acoustic emission data. Combined with the triaxial hydraulic fracturing experiment, the correlation between the microcrack onset position and the fracture pull-shear characteristics in the formation process of the hydraulic fracturing-induced fracture network was discussed entirely, which can effectively estimate the hydraulic fracturing effect. Zhang [105] conducted a volume fracture simulation study of a deep shale fracturing fracture network based on a 3D Wiremesh model. The results show that increasing construction time, improving construction displacement, and reducing fracturing fluid viscosity are conducive to increasing the volume of the fracturing fracture network and improving fracturing efficiency. Based on physical experiments and simulations, Abe et al. [106] found that the inter-fracture stress shadow effect is the main reason for affecting the effective fracture extension and the formation of a large-scale fracture network.

In sum, the above scholars have analyzed the influence of ground stress conditions, fracturing fluid properties, natural fracture properties, construction schemes, and other factors on the fracture mesh form through hydraulic fracturing experiments. Hydraulic injection fluid-driven hydraulic fracture formation joint mesh is

a dynamic and cyclic multi-scale process [107], which needs to comprehensively consider the influence of bore layout, ground stress, injection rate, reservoir medium properties, and other factors. In addition, to maximize the exploitation of reservoir resources, the best effect of hydraulic fracturing should be to form a complex fracture network system dominated by effective length hydraulic fracture [65]. In addition, to maximize the exploitation of reservoir resources, the best effect of hydraulic fracturing should be to form a complex fracture network system dominated by effective length hydraulic fracture. However, the actual engineering of hydraulic fracture-induced fracture network production is mainly based on experience and the lack of reliable fracturing theory based on the in-depth study of shale reservoir hydraulic fracturing fracture propagation and the formation mechanism of the complex fracture network. It is necessary to start the influence of confining pressure, water pressure, and physical and mechanical response characteristics of rock materials on the fracture network form, with the real-time monitoring and positioning of the deformation and acoustic emission signals on the rock through dynamic monitoring technologies such as high-precision displacement sensor and acoustic emission. By analyzing the characteristics of the time and frequency evolution of acoustic transmission signals, the microscopic (tension or shear) fracture response law of the process of hydraulic fracturing, combined with microscope observation and CT 3D reconstruction, the dynamic process of fracture network initiation, intersection propagation, and fracture network formation is finely characterized and the formation mechanism of complex fracture network is explained.

1.2.4 Existing Problems

According to the above research, scholars have carried out lots of detailed studies on the theory, experiment, and numerical simulation of the process of hydraulic fracture initiation, propagation, intersection and network formation involved in hydraulic fracture. The disturbance effect of the fracture network by fracturing parameters has also been discussed, but the current research work still faces the following problems:

- (i) The fracturing mechanism and model of the reservoir rock are mainly studied under constant pressurization rate or constant current injection conditions, while the breakdown process of rock under the perturbation of constant pressure and static fatigue in the fracture is relatively scarce. During the hydraulic fracturing segment construction, the hydraulic injection operation often needs to be repeated, and the inner wall of the wellbore will inevitably withstand the fatigue disturbance caused by continuous pressurization. Moreover, many physical experiments [22, 108, 109] have confirmed that when the fluid is applied to the rock for a long time at constant high pressure (60–95% P_b), the rock eventually breaks up and produces a relatively tortuous hydraulic fracture form. Studying the constant pressure fatigue fracture mechanism in the fracture

- is helpful to deeply understand the internal mechanism of rock hydraulic fracturing and improve the rock hydraulic fracture theory. The fracturing pressure of reservoir rock can be effectively reduced by adjusting the constant flow and pressure injection methods, and the fracturing operation cost can be saved.
- (ii) In the actual hydraulic fracture process, especially for pulse hydraulic fracture and fatigue hydraulic fracture, fluid pressure in the cracks is always fluctuating [110, 111]. However, the existing hydraulic fracturing theory does not consider the dynamic change of heterogeneous cloth fluid pressure effect caused by viscous flow and flow decay, which is limited by engineering applications [112, 113]. The heterogeneous distribution effect of the fluid pressure in the joint can better reflect the dynamic propagation law of the hydraulic fracture in the actual fracturing process.
 - (iii) At present, some progress has been made in studying the crack intersection mechanism of hydraulic approximation and fracture tip passivation, but the cognition of the critical transition state of the two processes is still not clear enough, and the predicted results of the criteria deviate significantly from the actual indoor experiments and engineering monitoring data [72, 114]; Considering the influence of fluid pressure, rock material, and mechanical properties of natural fracture, the composite criterion reflects the critical state of hydraulic and natural fracture, which is of great significance in analyzing the intersection of multiple fractures and predicting the formation of a complex fracture network.
 - (vi) High-pressure fluid-driven hydraulic fracture to form fracture mesh is a dynamic, cyclic multiscale process [107]. The current research on complex fracture mesh focuses on reflecting the fracturing effect and the characteristics of reservoir breakdown through the macroscopic fracture morphology while less considering the fracture evolution law of the hydraulic loading process and the fracture characteristics after the breakdown. In in-depth exploring the formation mechanism of complex sewing nets, it is necessary to consider the effects of well-laying tube layout, geographical stress direction, stress shadow effect of cracks, and changes like reservoir medium on the evolution of complex fracturing networks and morphological characteristics. To further explore the formation mechanism of complex fracturing nets, it is necessary to consider the effects of well-laying tube layout, geographical stress direction, stress shadow effect of fracture, and changes like reservoir medium on the evolution of complex fracturing networks and morphological characteristics [115,116].

References

1. Jiang TiX, Gu CG, Wang HY (2017) Shale gas horizontal well SRV fracturing technology. Science Press, Beijing. (in Chinese)
2. Ma X, Wang H, Zhou S et al (2021) Deep shale gas in China: geological characteristics and development strategies. Energy Rep 7(6):1903–1914

3. Zeng YJ, Yang CH, Zhang BP (2017) The theory and practice in shale gas development engineering. Science Press, Beijing. (in Chinese)
4. Yin PF (2020) Study on mechanical behavior and hydraulic fracturing mechanism of Longmaxi formation shale in Southern Sichuan Basin. China University of Mining and Technology
5. Zhao W, Jia A, Wei Y, Wang J, Zhu H (2020) Progress in shale gas exploration in China and prospects for future development. *China Petrol Explor* 25(01):31–44
6. Zhong D (2019) Numerical simulation research on the performance of fracturing horizontal well in shale gas reservoir. Southwest Petroleum University
7. He Z, Nie H, Hu D, Jiang T, Wang R, Zhang Y, Zhang G, Lu Z (2020) Geological problems in the effective development of deep shale gas: a case study of Upper Ordovician Wufeng-Lower Silurian Longmaxi formations in Sichuan Basin and its periphery. *Shiyou Xuebao/Acta Pet Sin* 41(04):379–391. <https://doi.org/10.7623/syxb202004001>
8. Ma Y, Cai X, Zhao P (2018) China's shale gas exploration and development: understanding and practice. *Pet Explor Dev* 45(04):561–574. [https://doi.org/10.1016/S1876-3804\(18\)30065-X](https://doi.org/10.1016/S1876-3804(18)30065-X)
9. Zhao J, Ren L, Jiang T, Hu D, Wu L, Wu J, Yin C, Li Y, Hu Y, Lin R, Li X, Peng Y, Shen C, Chen X, Yin Q, Jia C, Song Y, Wang H, Li Y, Wu J, Zeng B, Du L (2021) Ten years of gas shale fracturing in China: review and prospect. *Nat Gas Ind* 41(08):121–142
10. Pan L, Zhang Y, Cheng L, Lu Z, Kang Y, He P, Dong B (2018) Migration and distribution of complex fracture proppant in shale reservoir volume fracturing. *Nat Gas Ind B*. 38(05):61–70. <https://doi.org/10.1016/j.ngib.2018.11.009>
11. Jjiao F (2019) Theoretical insights, core technologies and practices concerning “volume development” of shale gas in China. *Nat Gas Ind B* 39(05):1–14. <https://doi.org/10.1016/j.ngib.2019.05.001>
12. Liu Z, Wang T, Gao Y, Zeng Q, Zhuang Z, Huang KC (2016) The key mechanical problems on hydraulic fracture in shale. *Guti Lixue Xuebao/Acta Mech Solida Sin* 37(1):34–49
13. Lee KS, Kim TH (2016) Integrative understanding of shale gas reservoirs. Springer, Heidelberg
14. Wang X, Wang P, Li Y, Lv M, Wei Y (2021) Research on the relationship between fracture volume density and shale gas productivity. *Geophys Prospect Pet* 60(05):826–833. <https://doi.org/10.3969/j.issn.1000-1441.2021.05.013>
15. Jia Y, Song C, Wang J, Gan Q (2021) The breakdown process of low-permeable shale and high-permeable sandstone rocks due to non-aqueous fracturing: the role of fluid infiltration. *J Nat Gas Sci Eng*. 89(4):103873. <https://doi.org/10.1016/j.jngse.103873>
16. Wang XL (2017) Numerical simulation of hydraulic fracturing in shale gas reservoirs based on the extended finite element method. University of Science and Technology of China
17. Sampath K, Perera M, Ranjith PG (2018) Theoretical overview of hydraulic fracturing breakdown pressure. *J Nat Gas Sci Eng* 58:251–265
18. Dou F, Wang JG, Leung CF, Ma Z (2021) The alterations of critical pore water pressure and micro-cracking morphology with near-wellbore fractures in hydraulic fracturing of shale reservoirs. *Eng Fract Mech* 242:107481. <https://doi.org/10.1016/j.engfracmech.2020.107481>
19. Huang RZ (1981) Initiation and propagation of hydraulically fractured fractures. *Petrol Explor Dev* 1981(05):62–74
20. Guo T, Zhang S, Liu W, Lai W (2013) Initiation pressure of multi-stage fracking for perforated horizontal wells of shale gas reservoirs. *Nat Gas Ind* 33(12):87–93. <https://doi.org/10.3787/j.issn.1000-0976.2013.12.013>
21. Sun K, Zhang S, Xin L (2016) Impacts of bedding directions of shale gas reservoirs on hydraulically induced crack propagation. *Nat Gas Ind B* 36(2):45–51. <https://doi.org/10.1016/j.ngib.2016.03.008>
22. Bungler AP, Lu G (2015) Time-dependent initiation of multiple hydraulic fractures in a formation with varying stresses and strength. *SPE J* 20(6):1317–1325
23. Bungler AP, Gordeliy E, Detournay E (2013) Comparison between laboratory experiments and coupled simulations of saucer-shaped hydraulic fractures in homogeneous brittle-elastic solids. *J Mech Phys Solids* 61(7):1636–1654. <https://doi.org/10.1016/j.jmps.2013.01.005>

24. Ma L, Fauchille AL, Chandler MR, Dowe P, Taylor KG, Mecklenburgh J, Lee PD (2021) In-situ synchrotron characterisation of fracture initiation and propagation in shales during indentation. *Energy* 215. <https://doi.org/10.1016/j.energy.2020.119161>
25. Le ZZ, Zhang GQ, Xing YK, Fan ZY, Zhang X, Kasperczyk D (2019) A laboratory study of multiple fracture initiation from perforation clusters by cyclic pumping. *Rock Mech Rock Eng* 52(3):827–840. <https://doi.org/10.1007/s00603-018-1636-5>
26. Rongved M, Holt RM, Larsen I (2019) The effect of heterogeneity on multiple fracture interaction and on the effect of a non-uniform perforation cluster distribution. *Geomech Geophys Geo-Energ Geo-Resour* 5:315–332
27. Zhu Y, Zhang H, Pan D, Zhai L, Gao S, Zhang Y, Chen C (2020) A case study on the optimal design of the horizontal wellbore trajectory for hydraulic fracturing in Nong'an oil shale. *Energies* 13(1):286. <https://doi.org/10.3390/en13010286>
28. Kumar D, Ghassemi A (2018) Three-dimensional poroelastic modeling of multiple hydraulic fracture propagation from horizontal wells. *Int J Rock Mech Min Sci* 2018:S1365160917310316. <https://doi.org/10.1016/j.ijmms.2018.01.010>
29. Zhang Z, Zhang S, Zou Y, Ma X, Li N, Liu L (2021) Experimental investigation into simultaneous and sequential propagation of multiple closely spaced fractures in a horizontal well. *J Pet Sci Eng* 202(1):108531. <https://doi.org/10.1016/j.petrol.2021.108531>
30. Hubbert M, Willis D (1957) Mechanics of hydraulic fracturing. *Transp Soc Petrol Eng AIME* 210:153–168
31. Haimson B, Fairhurst C (1976) Initiation and extension of hydraulic fractures in rocks. *Soc Petrol Eng J* 7(03):310–318
32. Rummel F, Winter RB (1983) Application of laboratory fracture mechanics data to hydraulic fracturing field tests. In: Nemat-Nasser S, Abé H, Hiraoka S (eds) *Hydraulic fracturing and geothermal energy. Mechanics of elastic and inelastic solids*, 5. Springer, Dordrecht
33. Ito T, Hayashi K (1991) Physical background to the breakdown pressure in hydraulic fracturing tectonic stress measurements. *Int J Rock Mech Min Sci* 28(4):285–293. [https://doi.org/10.1016/0148-9062\(91\)90595-D](https://doi.org/10.1016/0148-9062(91)90595-D)
34. Perkins TK, Kern LR (1961) Widths of hydraulic fractures. *J Pet Technol* 222(9):937–949. <https://doi.org/10.2118/89-pa>
35. Rummel F (1987) Fracture mechanics approach to hydraulic fracturing stress measurements. In: Atkinson BK (ed) *Fracture mechanics of rock*. Academic Press, London, pp 217–239
36. Zhang X, Wang JG, Gao F, Ju Y (2017) Impact of water, nitrogen and CO₂ fracturing fluids on fracturing initiation pressure and flow pattern in anisotropic shale reservoirs. *J Nat Gas Sci Eng* 45:291–306. <https://doi.org/10.1016/j.jngse.2017.06.002>
37. Morgenstern N (1962) A relation between hydraulic breakdown pressures and tectonic stresses. *Geofisica pura e applicata* 52(1):104–111
38. Lu G, Gordeliy E, Prioul R, Bungler A (2017) Modeling initiation and propagation of a hydraulic fracture under subcritical conditions. *Comput Methods Appl Mech Eng* 318:61–91. <https://doi.org/10.1016/j.cma.2017.01.018>
39. Gunarathna G, da Silva BG (2019) Influence of the effective vertical stresses on hydraulic fracture initiation pressures in shale and engineered geothermal systems explorations. *Rock Mech Rock Eng* 52(11):4835–4853
40. Chen Y, Ding Y, Liang C, Bai Y, Zhu D, Zou C (2021) An analytical model for fracture initiation of radial drilling-fracturing in shale formations. *Lithosphere* 1:3387123. <https://doi.org/10.2113/2021/3387123>
41. Michael A, Gupta I (2021) A comparative study of oriented perforating and fracture initiation in seven shale gas plays. *J Nat Gas Sci Eng* 88(4–5):103801
42. Fu Y (2019) The study on the rule of slick-water fracturing fluid flow in plugging of main fracture during the fracture of hydraulic fracturing. Xi'an Shiyou University
43. Griffith AA (1902) The phenomena of rupture and flow in solids. *Philosop Trans R Soc Math Phys Eng Sci* A221(4):163–198
44. Sneddon IN, Elliot HA (1946) The opening of a Griffith crack under internal pressure. *Q Appl Math* 4(3):262–267

45. Liu JZ, Wu XR (1997) Analytical expressions for crack opening displacements of edge cracked specimens under a segment of uniform crack face pressure. *Eng Fract Mech* 58(1):107–119
46. Hai TN, Lee JH, Elraies KA (2020) A review of PKN-type modeling of hydraulic fractures. *J Petrol Sci Eng*:107607
47. Wu Z, Cui C, Jia P, Wang Z, Sui Y (2021) Advances and challenges in hydraulic fracturing of tight reservoirs: a critical review. *Energy Geosci*. <https://doi.org/10.1016/j.engeos.2021.08.002>
48. Khalil MA, Susi AO (2020) Hydraulic fracture geometry modeling techniques for extracting unconventional reservoirs. *J Eng Res Rep* 5:1–5
49. Napier JAL, Detournay E (2019) Simulation of buoyancy-driven fracture propagation using the displacement discontinuity boundary element method. In: *Advances in engineering materials, structures and systems: innovations, mechanics and applications*, 525–530
50. Detournay E (2004) Propagation regimes of fluid-driven fractures in impermeable rocks. *Int J Geomech* 4(1):35–45
51. Detournay E, Hakobyan Y (2022) Hydraulic fracturing of weak rock during waterflooding. *Int J Numer Anal Meth Geomech* 46(2):416–435
52. Gao Y, Detournay E (2021) Hydraulic fracture induced by water injection in weak rock. *J Fluid Mechan* 927
53. Detournay E, Peirce AP, Bungler AP (2007) Viscosity-dominated hydraulic fractures. American Rock Mechanics Association
54. Garagash DI, Sarvaramini E (2012) Equilibrium of a pressurized plastic fluid in a wellbore crack. *Int J Solids Struct* 49(1):197–212
55. Zeng Y, Jin X, Ding S, Zhang B, Bian X, Shah S, McLennan J, Roegiers JC (2019) Breakdown pressure prediction with weight function method and experimental verification. *Eng Fract Mech* 214:62–78. <https://doi.org/10.1016/j.engfractmech.2019.04.016>
56. Li K, Smirnov NN, Pestov DA, Qi C, Kiselev AB (2020) An approximate analytical solution for hydraulic fracture opening under non-uniform internal pressure. *Mater Phys Mech* 44(3):288–305. https://doi.org/10.18720/MPM.4432020_2
57. Wrobel M, Papanastasiou P, Peck D (2022) A simplified modelling of hydraulic fractures in elasto-plastic materials. *Int J Fract*. <https://doi.org/10.1007/s10704-021-00608-w>
58. Ji Y, Wanniarachchi WAM, Wu W (2020) Effect of fluid pressure heterogeneity on injection-induced fracture activation. *Comput Geotech* 123:103589. <https://doi.org/10.1016/j.compgeo.2020.103589>
59. Ji Y, Yoon JS, Zang A, Wu W (2021) Mitigation of injection-induced seismicity on undrained faults in granite using cyclic fluid injection: a laboratory study. *Int J Rock Mech Min Sci* 146. <https://doi.org/10.1016/j.ijrmms.2021.104881>
60. Li Z, Elsworth D, Wang C (2021) Constraining maximum event magnitude during injection-triggered seismicity. *Nat Commun*. <https://doi.org/10.1038/s41467-020-20700-4>
61. Fang Z, Wu W (2022) Laboratory friction-permeability response of rock fractures: a review and new insights. *Geomechan Geophys Geo-Energy Geo-Resour* 8(1)
62. Wei M, Dai F, Ji Y et al (2021) Effect of fluid pressure gradient on the factor of safety in rock stability analysis. *Eng Geol* 12:106346. <https://doi.org/10.1016/j.engeo.2021.106346>
63. Shrivastava K, Hwang J, Sharma M (2018) Formation of complex fracture networks in the Wolfcamp Shale: calibrating model predictions with core measurements from the hydraulic fracturing test site. In: *SPE annual technical conference and exhibition*
64. Zhao J, Ren L, Shen C, Li Y (2018) Latest research progresses in network fracturing theories and technologies for shale gas reservoirs. *Nat Gas Ind B* 38(03):1–14. <https://doi.org/10.1016/j.ngib.2018.03.007>
65. Wang G, Yang D, Kang Z, Zhao J, Lv Y (2019) Numerical investigation of the in-situ oil shale pyrolysis process by superheated steam considering the anisotropy of the thermal, hydraulic, and mechanical characteristics of oil shale. *Energy Fuels* 33(12):12236–12250. <https://doi.org/10.1021/acs.energyfuels.9b02883>
66. Gao Y, Detournay E (2020) A poroelastic model for laboratory hydraulic fracturing of weak permeable rock. *J Mechan Phys Solids* 143

67. Renshaw CE, Pollard DD (1995) An experimentally verified criterion for propagation across unbounded frictional interfaces in brittle, linear elastic-materials. *Int J Rock Mech Min Sci Geo-Mechan Abstr* 32(3):237–249
68. Sarmadivaleh M, Rasouli V (2013) Modified Renshaw and pollard criteria for a non-orthogonal cohesive natural interface intersected by an induced fracture. *Rock Mech Rock Eng* 47(6):2107–2115
69. Zhang R, Li GS, Zhao ZH, Sheng M, Fan X, Chi HP (2014) New criteria for hydraulic fracture crossing natural fractures. *Yantu Gongcheng Xuebao/Chinese J Geotech Eng* 2014(3):585–588. <https://doi.org/10.11779/CJGE201403024>
70. Zhao HJ, Ma FS, Liu G, Guo J, Feng XL (2016) Influence of different scales of structural planes on propagation mechanism of hydraulic fracturing. *J Eng Geol*
71. Llanos EM, Jeffrey RG, Hillis R, Zhang X (2017) Hydraulic fracture propagation through an orthogonal discontinuity: a laboratory, analytical and numerical study. *Rock Mech Rock Eng* 50(8):2101–2118. <https://doi.org/10.1007/s00603-017-1213-3>
72. Yao Y, Wang W, Keer LM (2018) An energy based analytical method to predict the influence of natural fractures on hydraulic fracture propagation. *Eng Fract Mech* 189(2018):232–245
73. Zhao Y, He P, Zhang Y, Wang C (2019) A new criterion for a toughness-dominated hydraulic fracture crossing a natural frictional interface. *Rock Mech Rock Eng* 2018:1–13. <https://doi.org/10.1007/s00603-018-1683-y>
74. Zhao Y, Zhang YF, He PF (2019) A composite criterion to predict subsequent intersection behavior between a hydraulic fracture and a natural fracture. *Eng Fract Mech* 209:61–78. <https://doi.org/10.1016/j.engfracmech.2019.01.015>
75. Janiszewski M, Shen BT, Rinne M (2019) Simulation of the interactions between hydraulic and natural fractures using a fracture mechanics approach. *J Rock Mechan Geotech Eng* 11(6):1138–1150
76. Daneshy A (2019) Three-dimensional analysis of interactions between hydraulic and natural fractures. In: Society of petroleum engineers—SPE hydraulic fracturing technology conference and exhibition 2019, HFTC 2019
77. Zeng Y, Cheng W, Zhang X, Xiao B (2020) A criterion for identifying a mixed-mode I/II hydraulic fracture crossing a natural fracture in the subsurface. *Energy Explor Exploit* 38(6):2507–2520. <https://doi.org/10.1177/0144598720923781>
78. Zhu D, Du W (2022) A criterion for a hydraulic fracture crossing a frictional interface considering T-stress. *J Pet Sci Eng* 209. <https://doi.org/10.1016/j.petrol.2021.109824>
79. Zhao Z, Zhao Y, Jiang Z, Guo J, Zhang R (2021) Investigation of fracture intersection behaviors in three-dimensional space based on CT scanning experiments. *Rock Mech Rock Eng* 54(11):5703–5713. <https://doi.org/10.1007/s00603-021-02587-9>
80. Zheng P, Xia Y, Yao T, Jiang X, Xiao P, He Z, Zhou D (2022) Formation mechanisms of hydraulic fracture network based on fracture interaction. *Energy* 243:123057. <https://doi.org/10.1016/j.energy.2021.123057>
81. Chuprakov D, Melchaeva O, Prioul R (2014) Injection-sensitive mechanics of hydraulic fracture interaction with discontinuities. *Rock Mech Rock Eng* 47(5):1625–1640. <https://doi.org/10.1007/s00603-014-0596-7>
82. Blanton TL (1986) Propagation of hydraulically and dynamically induced fractures in naturally fractured reservoirs. In: Society of petroleum engineers—SPE unconventional gas technology symposium, UGT 1986
83. Warpinski NR, Teufel LW (1987) Influence of geologic discontinuities on hydraulic fracture propagation. *JPT J Pet Technol* 39(2). <https://doi.org/10.2118/13224-pa>
84. Chuprakov D, Prioul R (2015) Hydraulic fracture height containment by weak horizontal interfaces. In: SPE hydraulic fracturing technology conference, the Woodlands, Texas, USA
85. Xu W, Zhao J, Rahman SS, Li Y, Yuan Y (2019) A comprehensive model of a hydraulic fracture interacting with a natural fracture: analytical and numerical solution. *Rock Mech Rock Eng* 52:1095–1113. <https://doi.org/10.1007/s00603-018-1608-9>
86. Zhao K, Stead D, Kang H, Damjanac B, Donati D, Gao F (2020) Investigating the interaction of hydraulic fracture with pre-existing joints based on lattice spring modeling. *Comput Geotech* 122:103534. <https://doi.org/10.1016/j.compgeo.2020.103534>

87. Fu L, Shen R, Pang F, Yang H, Chen K (2019) Experiments on friction and non-steady slip for shale. *Diqiu Kexue - Zhongguo Dizhi Daxue Xuebao/Earth Sci J China Univ Geosci* 44(11):3783–3793. <https://doi.org/10.3799/dqkx.2019.189>
88. Wang R, Hu Z, Zhou T, Bao H, Wu J, Du W, He J, Wang P, Chen Q (2021) Characteristics of fractures and their significance for reservoirs in Wufeng-Longmaxi shale, Sichuan Basin and its periphery. *Oil Gas Geol* 42(06):1295–1306. <https://doi.org/10.11743/ogg20210605>
89. Jinzhou Z, Yongming L, Song W, Youshi J, Liehui Z (2014) Simulation of complex fracture networks influenced by natural fractures in shale gas reservoir. *Nat Gas Ind B* 34(01):68–73. <https://doi.org/10.1016/j.ngib.2014.10.012>
90. Zeng FH, Zhang T, Ma L, Guo JC, Zeng B (2021) Dynamic permeability model of volume fracturing network in deep shale gas reservoir and its application. *Nat Gas Geosci* 32(07):941–949. <https://doi.org/10.11764/j.issn.1672-1926.2021.04.001>
91. Dehghan AN, Goshtasbi K, Ahangari K, Jin Y (2015) Experimental investigation of hydraulic fracture propagation in fractured blocks. *Bull Eng Geol Environ* 74(3):887–895. <https://doi.org/10.1007/s10064-014-0665-x>
92. Sheng GL, Huang LY, Zhao H, Rao X, Ma JL (2021) Fracture network propagation and gas flow in shale gas reservoirs. *J Southwest Petrol Univ (Sci Technol Edn)* 43(05):84–96
93. de Pater CJ, Beugelsdijk LJJ (2005) Experiments and numerical simulation of hydraulic fracturing in naturally fractured rock. In: American rock mechanics association—40th US rock mechanics symposium, ALASKA ROCKS 2005: rock mechanics for energy, mineral and infrastructure development in the northern regions
94. Tan P, Jin Y, Han K, Hou B, Guo X, Gao J, Wang T (2017) Analysis of hydraulic fracture initiation and vertical propagation behavior in laminated shale formation. *Fuel* 206:482–493. <https://doi.org/10.1016/j.fuel.2017.05.033>
95. Zhao Z, Li X, He J, Mao T, Li G, Zheng B (2018) Investigation of fracture propagation characteristics caused by hydraulic fracturing in naturally fractured continental shale. *J Nat Gas Sci Eng* 53:276–283. <https://doi.org/10.1016/j.jngse.2018.02.022>
96. Chong Z, Yao Q, Li X (2019) Experimental investigation of fracture propagation behavior induced by hydraulic fracturing in anisotropic shale cores. *Energies* 12(976):1–16. <https://doi.org/10.3390/en12060976>
97. Jiang C, Niu B, Yin G, Zhang D, Yu T, Wang P (2019) CT-based 3D reconstruction of the geometry and propagation of hydraulic fracturing in shale. *J Pet Sci Eng* 179:899–911. <https://doi.org/10.1016/j.petrol.2019.04.103>
98. Wang J, Guo Y, Zhang K, Ren G, Ni J (2019) Experimental investigation on hydraulic fractures in the layered shale formation. *Geofluids* 4621038
99. Hou B, Chang Z, Fu W, Muhadas Y, Chen M (2019) Fracture initiation and propagation in a deep shale gas reservoir subject to an alternating-fluid-injection hydraulic-fracturing treatment. *SPE J* 24(4). <https://doi.org/10.2118/195571-PA>
100. Wu S, Li T, Ge H, Wang X, Li N, Zou Y (2019) Shear-tensile fractures in hydraulic fracturing network of layered shale. *J Pet Sci Eng* 183:106428. <https://doi.org/10.1016/j.petrol.2019.106428>
101. Chen Z, Li SM, Chen Z, Wang HT (2020) Hydraulic fracture initiation and extending tests in deep shale gas formations and fracturing design optimization. *Petrol Drilling Tech* 48(3):7
102. Dehghan AN (2020) An experimental investigation into the influence of pre-existing natural fracture on the behavior and length of propagating hydraulic fracture. *Eng Fract Mech*. <https://doi.org/10.1016/j.engfracmech.2020.107330>
103. Zhang H, Sheng JJ (2020) Numerical simulation and optimization study of the complex fracture network in naturally fractured reservoirs. *J Pet Sci Eng*. <https://doi.org/10.1016/j.petrol.2020.107726>
104. Wu S, Ge H, Wang X, Li T, Gao K (2021) Characterization and quantitative evaluation of hydraulic fracture network based on acoustic emission monitoring. In: 55th U.S. rock mechanics/geomechanics symposium 2021
105. Zhang W (2021) Deep shale hydraulic fracture network volume model and its application. *Oil Drill Product Technol* 43(01):97–103

106. Abe A, Kim TW, Horne RN (2021) Laboratory hydraulic stimulation experiments to investigate the interaction between newly formed and preexisting fractures. *Int J Rock Mech Min Sci* 141:104665. <https://doi.org/10.1016/j.ijrmms.2021.104665>
107. Li S, Li Y, Yang C, Zheng X, Wang Q, Wang Y, Li D, Hu W (2019) Experimental and numerical investigation of the influence of roughness and turbulence on LUT airfoil performance. *Acta Mech Sin Xuebao* 35(6):1178–1190. <https://doi.org/10.1007/s10409-019-00898-3>
108. Zhao Y, Zhang Y, Yang H, Liu Q, Tian G (2022) Experimental study on relationship between fracture propagation and pumping parameters under constant pressure injection conditions. *Fuel* 307. <https://doi.org/10.1016/j.fuel.2021.121789>
109. Zeng B, Lu D, Zou Y, Zhou J, Li S, Li N, Cao Z (2020) Experimental study of the simultaneous initiation of multiple hydraulic fractures driven by static fatigue and pressure shock. *Rock Mech Rock Eng* 53(11):5051–5067. <https://doi.org/10.1007/s00603-020-02190-4>
110. Zang A, Zimmermann G, Hofmann H, Niemz P, Kim KY, Diaz M, Zhuang L, Yoon JS (2021) Relaxation damage control via fatigue-hydraulic fracturing in granitic rock as inferred from laboratory-, mine-, and field-scale experiments. *Sci Rep* 11(1):6780. <https://doi.org/10.1038/s41598-021-86094-5>
111. Li Q, Wu X, Zhai C, Hu Q, Ni G, Yan F, Xu J, Zhang Y (2021) Effect of frequency and flow rate of pulsating hydraulic fracturing on fracture evolution. *Zhongguo Kuangye Daxue Xuebao/J China Univ Min Technol* 50(06):1067–1076
112. Jin W, Arson C (2020) Fluid-driven transition from damage to fracture in anisotropic porous media: a multi-scale XFEM approach. *Acta Geotech* 15:113–144. <https://doi.org/10.1007/s11440-019-00813-x>
113. Zheng H, Pu C, Sun C (2020) Numerical investigation on the hydraulic fracture propagation based on combined finite-discrete element method. *J Struct Geol* 130:1–8. <https://doi.org/10.1016/j.jsg.2019.103926>
114. Zhao Y, Zhang YF, Tian G, Wang CL, Bi J (2022) A new model for predicting hydraulic fracture penetration or termination at an orthogonal interface between dissimilar formations. *Pet Sci* 19(6):2810–2829. <https://doi.org/10.1016/j.petsci.2022.08.002>
115. Zhao J, Ren L, Hu Y (2013) Controlling factors of hydraulic fractures extending into network in shale formations. *Xinan Shiyou Daxue Xuebao/J Southwest Pet Univ* 35(01):1–9. <https://doi.org/10.3863/j.issn.1674-5086.2013.01.001>
116. Zhang Y, Long A, Zhao Y, Zang A, Wang C (2023) Mutual impact of true triaxial stress, borehole orientation and bedding inclination on laboratory hydraulic fracturing of Lushan shale. *J Rock Mech Geotech Eng*. <https://doi.org/10.1016/j.jrmge.2023.02.015>

Open Access This chapter is licensed under the terms of the Creative Commons Attribution 4.0 International License (<http://creativecommons.org/licenses/by/4.0/>), which permits use, sharing, adaptation, distribution and reproduction in any medium or format, as long as you give appropriate credit to the original author(s) and the source, provide a link to the Creative Commons license and indicate if changes were made.

The images or other third party material in this chapter are included in the chapter's Creative Commons license, unless indicated otherwise in a credit line to the material. If material is not included in the chapter's Creative Commons license and your intended use is not permitted by statutory regulation or exceeds the permitted use, you will need to obtain permission directly from the copyright holder.

